ACCEPTED MANUSCRIPT
Originally published in:
International Journal of Adhesion and Adhesives, Vol. 98, Paper No. 102550 (2020)
https://doi.org/10.1016/j.ijadhadh.2020.102550
https://www.sciencedirect.com/science/article/abs/pii/S0143749620300105

REINFORCED BIOBASED ADHESIVE FOR ECO-FRIENDLY SANDWICH PANELS

Pablo Resende Oliveira[1,2], Michael May[1], Tulio Hallak Panzera[3*], Fabrizio Scarpa[4], Stefan Hiermaier[1,2]

[1] Fraunhofer EMI, Ernst-Mach Institut, Freiburg im Breisgau, Germany.

[2] Institute of Sustainable Systems Engineering, Albert-Ludwigs Universität Freiburg, Freiburg im Breisgau, Germany.

[3] Centre for Innovation and Technology in Composite Materials (CIT^{e}C), Department of Mechanical Engineering, Federal University of São João del Rei (UFSJ), Brazil.

Corresponding author[*]: panzera@ufsj.edu.br

[4] Bristol Composites Institute (ACCIS), University of Bristol, UK

Abstract: *This work describes the development of a bio-polyurethane (bio-PU) adhesive made from castor oil plant to be used in sustainable (eco-friendly) sandwich panels made from recycled plastic waste. Low-cost fillers, such as Portland cement and recycled rubber particles are incorporated into the biopolymer to modify its mechanical behaviour. Epoxy is also used to benchmark the mechanical performance of the reinforced biopolymer described in this work. A full factorial design is performed to identify the effects of the types of adhesive, particles and their weight fraction on the mechanical and physical properties of hybrid panels. Single lap and adapted T-peel tests are used to assess the adhesion of the polymers to the aluminium surfaces. The inclusion of 3 wt% cement particles in the biopolymer provides a significant increase in the tensile strength and stiffness compared to the pristine bio-PU. Other properties that benefit from that amount of reinforcement in the bio-adhesive are the impact resistance and reduction of density and porosity compared to higher fractions of inclusions. Despite its lower mechanical properties, the biopolymer with rubber particles provides however an increase of the single lap shear strength, the opposite of what happens when using the reinforced epoxy polymer. The T-peel test also highlights the higher bonding affinity of the biopolymer to the sustainable sandwich core; that indicates the promise of using this biopolymer-reinforced adhesive in secondary and sustainable applications.*

Keywords: biopolymer, sustainable structures, Design of Experiment, peel strength, recyclability.

1. Introduction

Bonding by adhesive is a widely used technique to assemble components because of its intrinsic high bonding strength by unit weight, reduced stress concentrations, uniform load distribution and affinity to several substrates. The drawbacks of joining by adhesive are however the long curing times, the need for surface preparation and the effect of moisture and temperature on their durability. Another critical aspect for adhesives is the strong influence of the bonding properties on the structural performance of the component. Two techniques used to improve the adhesive bonding to the substrate

consist in the use of a proper surface treatment, and the inclusion of fillers in the adhesive to enhance the strength and deformation behaviour during loading. While surface treatments are in general expensive and require increased workload and time, fillers can be easy to disperse into the polymer. In particular, the dispersion of nanoparticles has provided some promising results for an effective enhancement of the bonding performance. Saraç *et al.* [1] have evaluated the inclusion of three types of oxide nanoparticles (Al_2O_3, TiO_2, SiO_2) in epoxy polymer by single lap joints testing under quasi-static and fatigue loads. The Authors have observed that the particles prevent the formation and propagation of cracks, leading to an increase of the tensile strength up to 97% compared to the neat epoxy. Zhou *et al.* [2] said that silica nanoparticles also enhanced the thermal stability and the resistance of epoxy polymer against severe conditions (100% relative humidity and 60°C). Jojibabu *et al.* [3] reported that carbon nanotubes (CNTs) significantly increased the lap shear strength (up to 53%) of reinforced epoxy adhesives with low particle inclusions (limited to 1 wt%); this was attributed to the high CNTs modulus and good dispersion in the polymer. Larger amounts of nanoparticles tend to increase the viscosity of the adhesive, limiting the presence of a homogeneous particles distribution and the effective reinforcement of the adhesive. Graphene nanoparticles (GNPs) triggered a 53% increase in energy absorption compared to neat epoxy polymer cases according to Scarselli *et al.* [4]. Another approach considered in open literature is related to the simultaneous use of stiff and soft particles, such as carbon nanoparticles and micro rubber respectively. Quan *et al.* [5] added graphene nanoplatelets up to 0.5 wt% to rubber-modified epoxy (10 vol%), leading to a marginal increment in tensile modulus and a 21% increase in fracture energy. In contrast, little focus has been placed on the use of low-cost microparticles as fillers in adhesives. Micro-fillers are easier to work with, tend to exhibit a facile interaction with the polymer and constitute a possible recycling alternative as disposed particles from high-end structures. Santana *et al.* [6] have evaluated the use of microparticles (silica particles and Portland cement) within the epoxy polymer adhesive in a co-cured single lap joint of glass fibre reinforced polymer. The single lap strength was increased by 36% with the use of cement, and this was attributed to the interlocking effect with the glass fibre fabric and the stiffening of the matrix.

Sustainability is also a recent concern in automotive and construction engineering applications. The reduction of unsustainable and harmful materials is nowadays a relevant objective. Petroleum-based polymers are the most widely applied commercial adhesives, however, they are not biodegradable and may release toxic fumes during curing as indicated by Packham [7]. Several ecological, non-toxic, low-cost and renewable alternatives for adhesive bonding have however emerged in recent years based on biopolymers. Biopolymers may provide good chemical resistance, fast curing, and satisfactory early green strength (adhesive strength before full cure). The reduced mechanical performance of biopolymers is however a challenge for the broadening of the applications of plant-based adhesives. One of the most versatile bio-sources of potentially green adhesives is castor bean plant due to its low cost, abundance and non-toxicity. Moghadam *et al.* [8] developed a high strength castor oil-based polyurethane (PU) with improved isocyanates that possess higher affinity with wood substrates. The substrate type plays

an important role in the bonding strength of castor oil-based polymers. Bio-PU adhesives on metal and wood surfaces achieved a strong bonding with polyethylene (PE) because of the presence of electrostatic mechanisms and hydrogen bonds, as shown by Tenorio-Alfonso *et al.* [9]. Fillers have also been incorporated to increase the strength and toughness of biobased adhesives. Malik and Kaur [10] have tested the dispersion of TiO_2 in biobased PU from castor oil at different quantities (1 to 5 wt%). The inclusion of 3 wt% TiO_2 led to increased shear strength and accelerated curing, with 70% of the full strength achieved after one day of cure. Panchireddy *et al.* [11] also studied the effect of SiO_2 and ZnO fillers on the lap shear strength and water absorption of soybean oil PU. Functionalized fillers helped to reduce the water absorption to a reasonable value (around 4%) and increased the stiffness of the adhesive and its shear strength up to 173% from pristine polyurethane by using ZnO dispersions.

The literature review highlights the potential of using biopolymer-based adhesives on different surfaces from wood to metals. The use of these biopolymers can be promising for sustainable sandwich structures, especially those made from recycled components investigated by Oliveira *et al.* [12,13]. The latter referenced works [12,13] describe the use of synthetic thermoset polymer for bonding the aluminium skins, while the core consisted of discarded bottle caps. These sustainable panels can be applied in a variety of fields, such as the replacement of secondary structures in vehicles (cargo-bay or truck floors), as advertisement panels, and in the construction industry (split walls or lightweight infrastructure, e.g. containers). Replacing the synthetic adhesive with a biobased one can improve the sustainability of these eco-designed panels. It is however worth mentioning that the reduced mechanical performance of biobased polymers is a limitation for the structural integrity of these panels. In addition, the environmental impact of these biobased adhesives needs to be better determined by relevant methods such as a life cycle assessment. In this context, as a first step towards the use of biobased adhesives in sandwich panels, this work aims to characterise the mechanical performance of a particular bio-polyurethane from castor oil plant reinforced with Portland cement and recycled rubber particles. Rubber particles are a valuable filler for composite materials because they help to increase the energy absorption and the damping ratio in composites according to Ribeiro Filho *et al.* [14]. In this work a full factorial design ($2^2 3^1$) is performed to identify the effects of type of particle (rubber and cement particles), amount of inclusions (3, 6, and 10 wt%) and type of polymer used (biobased and epoxy) on the physical and mechanical properties of reinforced polymer composites. Adhesion tests to relevant substrates such as aluminium and bottle cap are also performed to better understand the potential use of biobased polymer in the manufacture of sustainable panels consisted of recycled bottle caps core and future analysis of product impact [12,13].

2. Materials and Methods

2.1 Materials

Bio-polyurethane based on castor oil (AGT 1315) was supplied by Imperveg Company (Brazil). This biopolymer is a bi-component adhesive consisting of prepolymer and polyol mixed with 1:1.2 by

weight. The polyol is synthesised from the castor oil plant – *Ricinus Communis*, in which a tri-functional polyester is obtained. Polyol is derived from the transformation of diphenylmethane diisocyanate and fatty acids. The components of the epoxy system are Renlan-M, a bisphenol A-(epichlorhydrin) resin, and HY956, a triethylenetetramine hardener, both supplied by Huntsman (Brazil). The resin/hardener ratio is 5:1. Aluminium sheets, type AW-5754 (Figure 1a), with 1.5 mm thickness, are used in single lap and T-peel bond tests. Coca-Cola™ plastic bottle caps made of high density polyethylene (Figure 1.b) are also evaluated for bonding tests. Bottle caps are carefully washed and dried at room temperature for 24 hours without further surface treatment. Bottle caps were characterised in a previous study [12], in which approximate strength (50 MPa) and stiffness (1.01 GPa) were determined. The rubber particles were collected at a local tyre remoulding company in Brazil, washed and sieved at a particle size range of 50/100 US-Tyler (149-297 µm). Portland cement (ASTM III type) manufactured by Holcim/Lafarge (Brazil) was used as received.

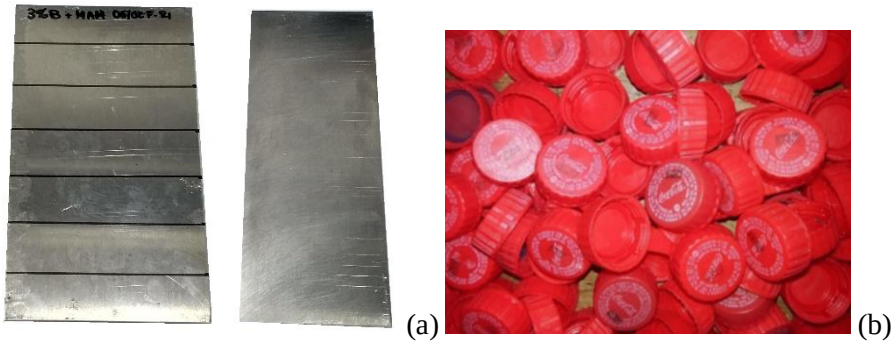

(a) (b)

Figure 1. Aluminium skins for single lap (175 × 100 mm^2) and T-peel tests (175 × 70 mm^2) (a) and plastic bottle caps (b) used in this research.

2.2 Full factorial design

A $2^2 3^1$ full factorial design investigates the effect of the type of adhesive (bio-polyurethane from castor oil and epoxy polymer), particle filler (recycled rubber particles and cement particles) and quantities of particles used (3, 6 and 10 wt%) on the tensile, impact, apparent density, porosity and water absorption properties of the reinforced polymers. Reference samples of the pristine polymers (bio-polyurethane from castor oil and epoxy polymer) are manufactured for physical and mechanical characterisation. Other factors kept constant are the polymer mixing ratio (5:1 in epoxy and 1:1.2 for bio-polyurethane), the mixing time (2 minutes) and the curing conditions (28 days at room temperature ~25°C, ~55% RH). Table 1 shows the twelve experimental conditions and two non-reinforced references. At least four (4) samples were produced per condition and per replicate for each proposed test, with two (2) replicates of each condition, resulting in, at least, eight (8) experimental samples per tested condition.

The Analysis of Variance (ANOVA) is used to identify the effects of factors and/or interactions on responses when considering a 95% of confidence interval, as stated by Montgomery [15]. Interaction

between factors occurs when the effect of one factor on a particular response is dependent of the level of another factor. When an interaction effect is significant, the individual factors can be interpreted jointly. The indicator of the significance of factors and interactions within the confidence interval is a P-Value of 0.05 or less. The Minitab v.18 software has been used to manipulate the data obtained in this work.

Table 1. Full factorial design ($2^2 3^1$) with unreinforced references for adhesive characterisation tests.

Condition	Type of Polymer	Type of Particle	Amount of Particles (wt%)
REF. 1	Epoxy	-	-
REF. 2	Biopolymer	-	-
C1	Epoxy	Cement	3
C2	Epoxy	Cement	6
C3	Epoxy	Cement	10
C4	Epoxy	Rubber	3
C5	Epoxy	Rubber	6
C6	Epoxy	Rubber	10
C7	Biopolymer	Cement	3
C8	Biopolymer	Cement	6
C9	Biopolymer	Cement	10
C10	Biopolymer	Rubber	3
C11	Biopolymer	Rubber	6
C12	Biopolymer	Rubber	10

This adhesive characterisation has shown the most appropriate parameters for subsequent adhesion tests (single lap tests and Cap T-peel test), considering the combination of high strength and impact resistance, low density and polymer porosity. Only one amount of particles (3 wt%) has been therefore considered. A full factorial design (2^2) consisting only of the types of polymer and particles has been carried out. The six conditions are given in Table 2, including the ones related to the polymers in pristine conditions. Aside from the 3 wt% of particles, the type and thickness of the bonding substrate (type AW-5754 aluminium skin with 1.5 mm thickness) are the other constant factors of the Design of Experiment (DoE) performed here.

Table 2. Full factorial design (2^2) with references for bonding characterisation.

Type of Polymer	Type of Particle	Amount of Particle (wt%)
Epoxy	-	-
Epoxy	Cement	3
Epoxy	Rubber	3
Biopolymer	-	-
Biopolymer	Cement	3
Biopolymer	Rubber	3

2.3 Manufacturing and testing

2.3.1 Characterisation of the adhesive

The samples of the reinforced adhesive polymers are produced by a manual mixing process lasting at least 2 minutes to allow the full dispersion of the particles within the polymer without air bubbles. Polymer hardener is added to the mixture and poured into custom silicone moulds made for each type of test considered: dog-bone samples (Figure 2a) for tensile tests according to ASTM D638 [16], prismatic samples (see Figure 2b) for Charpy impact (ASTM D6110 protocol [17]) and cylindrical samples (see Figure 2c) for physical properties (apparent density, apparent porosity, and water absorption) following the ASTM C20 guidelines [18]. A Shimadzu AGX-100 testing machine with 100 kN load cell and a 2 mm/min crosshead speed is used. Energy absorption data are obtained from a Jinjian impactor type XJJ-50 Series. The cylindrical samples are weighted after oven-drying them for 1 hour by using a precision scale. The specimens are then immersed in water under vacuum pressure for 24 h. The submersed weight and the saturated weight of the samples are recorded to calculate the properties. The morphology of the reinforced adhesives is investigated by backscatter electron images using Hitachi T-3000 scanning electronic microscope (SEM) operating at 15kV.

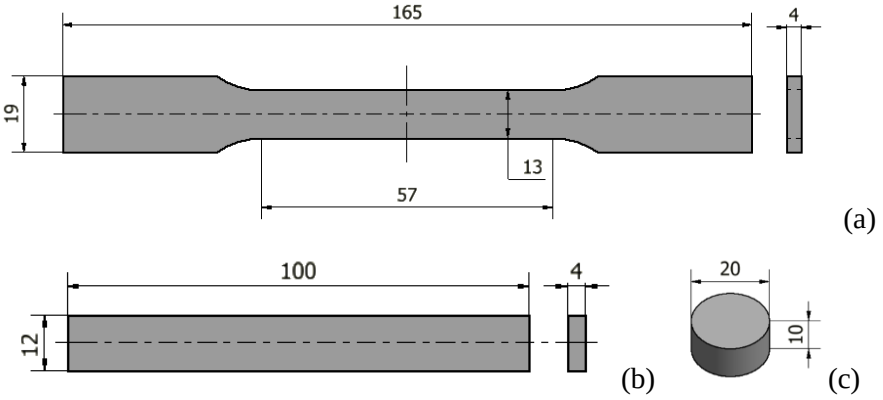

Figure 2. Sample dimensions (in millimetre) for tensile (a), impact (b), and physical (c) tests.

2.3.2 Single lap joint Test

The bond strength of unfilled and filled adhesives deposited to the aluminium substrate is determined by single-lap shear testing according to ASTM D1002 [19]. The aluminium skins of 102 × 175 mm^2 received a surface treatment based on initial degreasing with liquid detergent, with subsequent sanding of the contact area using a 150-grit at ± 45° direction. In addition, the metal surface is thoroughly cleaned with acetone and dried. After treatment, a thin layer of adhesive is spread over the surfaces, which are overlapped to a length of 12.7 mm (Figure 3a) and estimated constant thickness in all samples of 0.2 mm. A constant weight-pressure of 3 kPa is applied to the contact to expel the excess of adhesive and create a uniform thin adhesive layer. A metallic support on the upper skin is applied to keep it horizontal, making the skins parallel to each other and preventing plate eccentricity. After the curing period, individual single lap joint samples (Figure 3b) are obtained from the plate using a band saw

(Makita LB1200F), and the surfaces of the overlapping side are discarded (as recommended by the standard). Five (5) samples are produced per replicate for each of six (6) experimental conditions. Two (2) replicates are adopted, resulting in 60 specimens for this particular test. Metal end tabs are added to samples prior to testing. A Shimadzu test machine is used at a speed of 1 mm/min and a 100 kN load cell. The maximum shear load and apparent shear strength are based on the stress in the overlap area, and the apparent shear stiffness is obtained by the slope of the linear force vs. displacement curve, ranging from 50 and 200 N, which also agrees with the load range reported by Santana *et al.* [6].

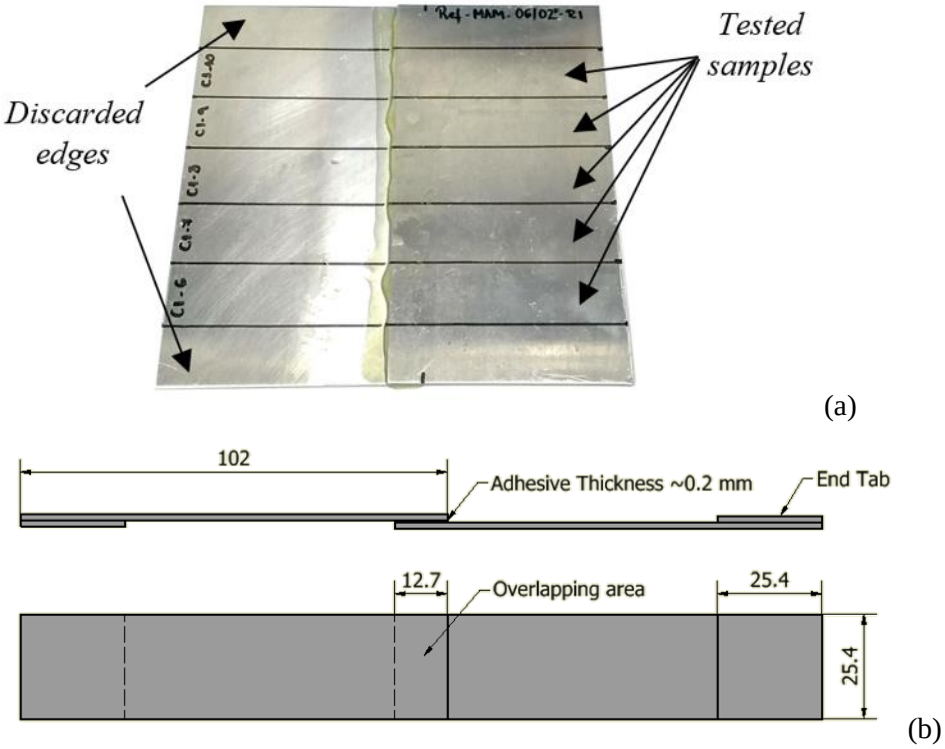

Figure 3. Single lap manufactured plates (a) and diagram of individual sample with dimensions in millimetres (b).

2.3.3 T-peel test

An adapted T-peel test is performed here to assess the bonding condition between the aluminium skins and the bottle caps used in previous sandwich panel structures [12,13]. T-peel samples (Figure 4) are fabricated in a similar procedure to previous works by Oliveira *et al.* [12,13]. Aluminium skins of 180×70 mm^2 are covered by a release film to limit the length of the bonding surface as shown in Figure 4a. The adhesive is spread over the aluminium bonding area, with subsequent contact of the caps on the first skin. Two alternated caps are placed next to each other to form a T-peel sample (Figure 4b). The mould is closed and a uniaxial pressure of 3.5 kPa is applied for 24 hours. The second skin is bonded following the same procedure described above. An upper skin holder at the same height as the bottle caps is placed in the non-bonded area to ensure that the skins are parallel to each other. Three sandwich specimen are considered for each condition. A band saw is used to cut the sandwich specimens to obtain individual T-peel samples. The L-brackets are riveted into the sample, and this allows an easy grip to

the machine during tensile loading (Figure 4c). A Shimadzu AGX testing machine equipped with a 100 kN load cell is used to perform the tests at 4 mm/min. Three (3) samples are produced for each experimental condition and replicate. The dimensions of the bonding surfaces followed the guidelines provided by Mousa *et al.* [20].

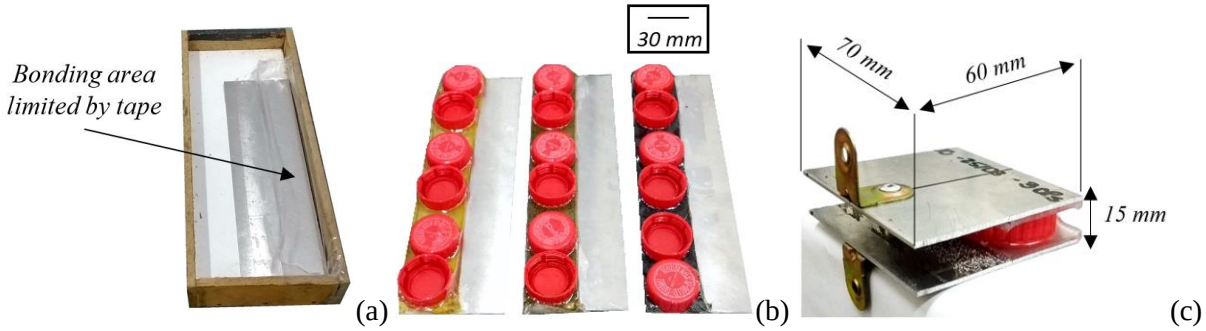

Figure 4. Manufacturing mould (a), caps attached to first skin (b) and manufactured T-peel sample (c).

3. Results:

3.1 Characterisation of the adhesive

3.1.1 Mechanical properties

The statistics related to the tensile and impact properties are shown in Table 3. Standard deviations are all limited to the 11% of the averages. Table 5 shows the ANOVA results for the mechanical properties. P-Values below 0.05 are highlighted in bold, while higher order significant effects are also underlined. The values of R^2 vary between 99.14 and 99.68%, which indicate an excellent correspondence of the model to the real experiments. In order to validate ANOVA, data should follow the normal distribution [15]. The Anderson-Darling normality test has been therefore performed and P-Values of 0.05 or greater have been observed in all responses (Table 4).

Table 3. Mechanical properties of epoxy polymer and biobased polymer.

Type of Polymer	Type of Particle	Amount of Particle (wt%)	Young's Modulus (GPa)			Tensile Strength (MPa)			Impact Resistance (kJ/m²)		
			Mean	SD	CV	Mean	SD	CV	Mean	SD	CV
Epoxy	-	-	1.9	0.2	7.9%	30.8	2.5	8.2%	15.6	1.0	6.5%
	Cement	3	2.6	0.2	8.0%	37.9	3.2	8.3%	12.3	0.9	7.0%
	Cement	6	2.1	0.2	10.7%	34.1	3.1	9.0%	13.1	1.0	7.8%
	Cement	10	2.3	0.2	10.5%	34.4	3.2	9.4%	8.3	0.7	8.3%
	Rubber	3	1.6	0.2	9.3%	27.6	1.5	5.4%	7.0	0.8	10.7%
	Rubber	6	2.0	0.2	9.9%	26.8	1.7	6.4%	9.0	0.4	4.9%
	Rubber	10	1.6	0.1	8.3%	23.7	2.6	11.1%	7.6	0.4	5.8%
Biopolymer	-	-	0.4	0.0	10.4%	11.1	0.3	2.7%	8.5	1.0	11.3%
	Cement	3	1.3	0.1	3.9%	18.0	0.8	4.6%	18.5	1.3	6.7%
	Cement	6	1.0	0.1	6.9%	17.6	0.8	4.3%	13.4	1.1	8.2%
	Cement	10	1.0	0.1	8.4%	16.1	0.8	4.8%	12.0	0.5	4.2%
	Rubber	3	0.3	0.0	10.9%	7.3	0.8	11.5%	11.3	0.5	4.6%
	Rubber	6	0.1	0.0	5.3%	3.9	0.4	10.2%	8.4	0.4	5.1%
	Rubber	10	0.1	0.0	2.8%	2.1	0.3	13.1%	7.9	0.5	5.8%

SD = standard deviation and CV = coefficient of variation

Table 4. Analysis of Variance (DoE) for the mechanical properties.

	Factors and Interactions	Tensile Test		Impact test
		Tensile strength	Young's Modulus	Impact Resistance
P-Value ≤ 0.05	Type of Polymer (TPo)	**0.000**	**0.000**	**0.000**
	Type of Particle (TPa)	**0.000**	**0.000**	**0.000**
	Amount of Particle (AP)	**0.000**	**0.000**	**0.000**
	TPo*TPa	**0.004**	**0.000**	**0.000**
	TPo*AP	0.935	0.116	**0.000**
	TPa*AP	0.217	**0.000**	**0.000**
	TPo*TPa*AP	**0.047**	**0.000**	**0.000**
R^2 (adj)		99.14%	99.54%	99.68%
AD (P-Value ≥ 0.05)		0.630	0.980	0.573

The tensile strength and the modulus are affected by a third order interaction effect (Table 5 and Figure 5). The dashed red lines indicate the reference polymers in pristine condition (without reinforcement). A Tukey´s test has been used to compare the means. Averages that do not share a letter (shown near each value in Figure 5) are statistically different [15]. Epoxy polymer (Groups A and B) exhibits higher strength and modulus than biopolymer (Groups C and D) for all conditions tested (Figure 5a and 5b, plots i and ii). The biopolymer however is more susceptible to the reinforcing effect of the filler. In general, dispersions of cement particles into epoxy lead to a slight increase in the tensile strength and modulus (limited to 15% in strength and 22.5% in stiffness). In contrast, cement-based biopolymer exhibit a significant increase in tensile strength (around 55%) and modulus (up to 183%). The incorporation of rubber reduces the tensile properties of the two types of polymers, especially in the case of biopolymer. These findings also indicate the presence of a high reactivity of the bio-polyurethane with the fillers. The highest values of tensile properties are achieved by using a 3 wt% inclusion of the two types of particles. The use of a 10 wt% dispersion leads however to mechanically weaker polymer, mainly when the rubber is used. A 3 wt% of cement particles provides a 97% increase in tensile strength and almost 130% in tensile modulus (Figure 5a and 5b, plot iii).

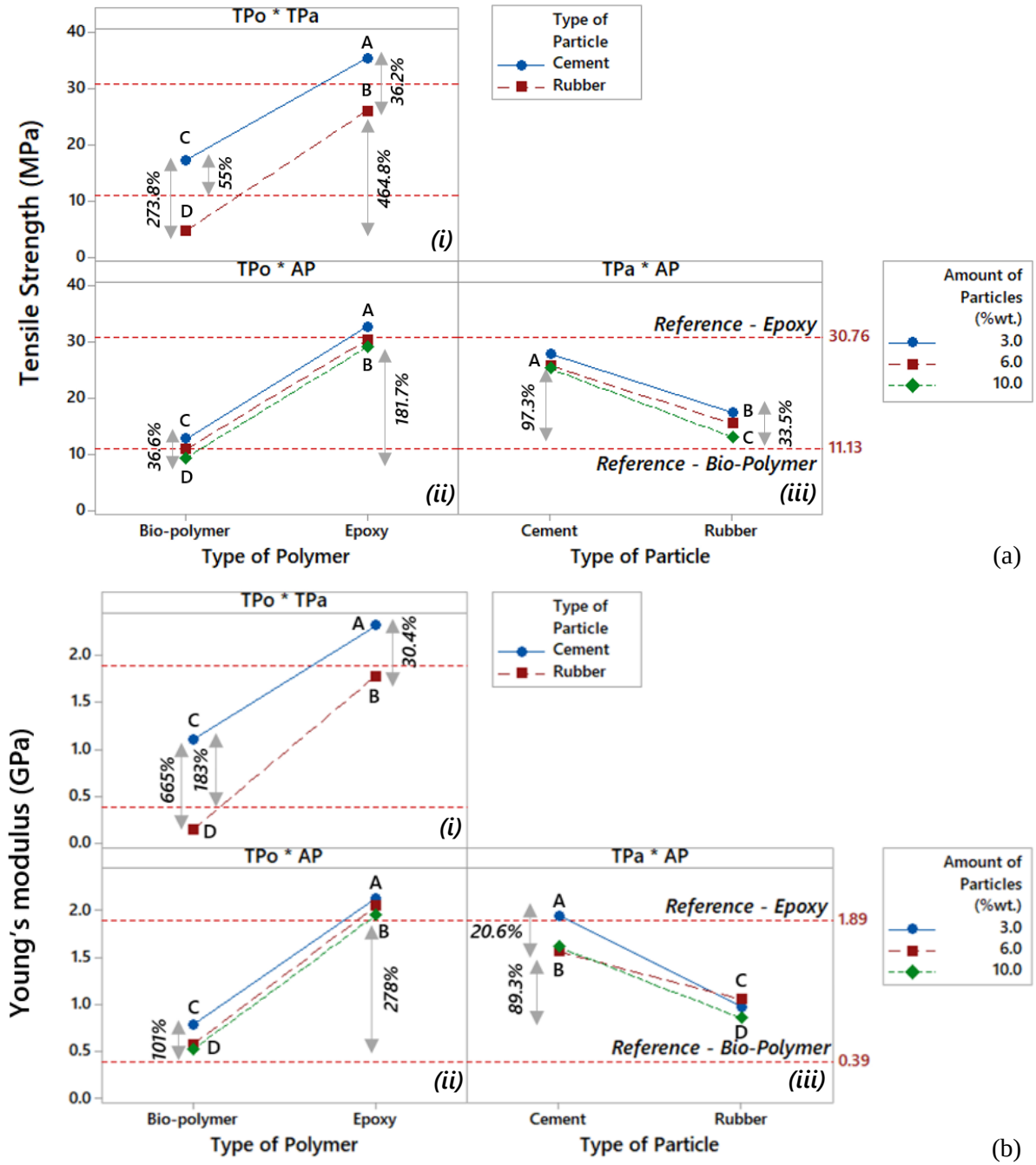

Figure 5. Third order interaction plots for the tensile strength (a) and the stiffness (b)

The impact resistance is also affected by a third-order interaction effect (Figure 6). Epoxy polymer in pristine condition shows an 82% higher resistance than pristine biopolymer. Nevertheless, the impact resistance appears to be mostly affected by the presence of particles. Cement particles provide a 72% increase in impact resistance over unreinforced biopolymer, being 39% higher than the reinforced epoxy. In contrast, the reinforced epoxy polymer shows reductions in impact resistance, 28% for cement and 50% for rubber particles, as shown in Figure 6, plot i. The highest impact resistance in reinforced polymers is obtained when 3 wt% and 6 wt% of particles are added to biopolymer and epoxy, respectively. Larger weight loadings of particles deteriorate the properties (Figure 6, plot ii). Biopolymer shows however a significant increase of the impact resistance even when 10 wt% of particles are used,

compared to the pristine polymer. The interaction effect between the types and quantities of particles shown in Figure 6 (plot iii) shows that the use of 3 wt% of cement provides the greatest impact resistance. No significant change is found when 3 wt% and 6 wt% of rubber are dispersed. A further increase of rubber weight loading (10 wt%) leads to an overall reduction of the properties by approximately 15%.

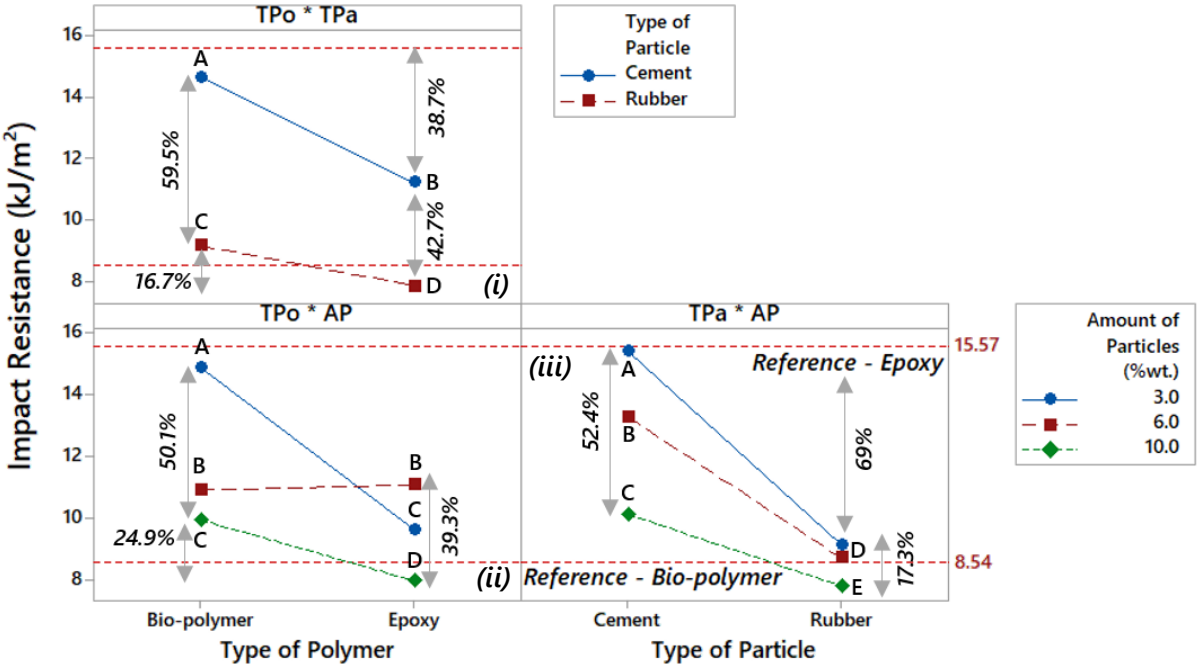

Figure 6. Third order interaction plot for impact resistance.

3.1.2 Physical Properties

Table 5 shows the physical properties for each experimental condition. The standard deviation and the coefficient of variation indicate small variations in the mean values. The ANOVA results are presented in Table 6. All properties are statistically affected by third order interaction effects with P-Values less than 0.05 (Table 6). Figure 7 shows the plots of the interaction effects including the reference values of each polymer. Epoxy polymer does not show detectable porosity, nor water absorption in pristine condition. No reference line for the epoxy is therefore shown in Figures 7b and 7c. The values of R^2 (adj) display an excellent adjustment of the experimental data to the statistical model. The P-Values obtained by the Anderson Darling test are greater than 0.05 for all considered properties, and this ensures the normality condition of the analysed data.

Table 5. Results of physical properties for epoxy polymer and biobased polymer conditions

Type of Polymer	Type of Particle	Amount of Particle (wt%)	Apparent Porosity (%)			Water Absorption (%)			Apparent Density (g/cm³)		
			Mean	SD	CV	Mean	SD	CV	Mean	SD	CV
Epoxy	-	-	-	-	0.0%	-	-	0.0%	1.2	2.9E-03	0.2%
	Rubber	3	0.5	1.2E-03	0.2%	0.4	1.7E-03	0.4%	1.2	2.0E-03	0.2%
	Rubber	6	1.0	1.6E-02	1.5%	0.9	1.2E-02	1.3%	1.2	2.7E-03	0.2%
	Rubber	10	1.1	2.9E-03	0.3%	0.9	8.6E-03	0.9%	1.2	1.4E-02	1.2%

	Cement	3	0.5	4.0E-03	0.8%	0.4	2.8E-03	0.6%	1.2	1.7E-03	0.1%
	Cement	6	1.1	1.3E-03	0.1%	1.0	2.2E-03	0.2%	1.2	1.5E-03	0.2%
	Cement	10	1.5	1.1E-02	0.8%	1.3	8.3E-03	0.6%	1.2	1.4E-03	0.1%
Biopolymer	-	-	2.2	7.3E-02	3.3%	2.1	7.9E-02	3.8%	1.1	4.7E-03	0.4%
	Rubber	3	3.0	1.1E-02	0.4%	2.3	3.5E-02	1.5%	0.8	9.1E-03	1.1%
	Rubber	6	22.3	7.7E-03	0.0%	12.7	1.6E-02	0.1%	0.6	3.1E-04	0.0%
	Rubber	10	28.7	4.8E-02	0.2%	21.7	3.0E-02	0.1%	0.7	9.4E-04	0.1%
	Cement	3	1.1	1.3E-02	1.2%	1.0	5.5E-03	0.5%	0.9	1.3E-02	1.4%
	Cement	6	1.9	3.5E-02	1.8%	1.8	1.7E-03	0.1%	0.9	1.4E-02	1.5%
	Cement	10	2.0	4.6E-02	2.3%	1.9	3.3E-02	1.7%	0.9	5.2E-03	0.6%

SD = standard deviation and CV = coefficient of variation

Table 6. DoE Results for the tested conditions

Factors and Interactions		**Apparent Porosity**	**Water Absorption**	**Apparent Density**
P-Value ≤ 0.05	Type of Polymer (TPo)	**0.000**	**0.000**	**0.000**
	Type of Particle (TPa)	**0.000**	**0.000**	**0.000**
	Amount of Particle (AP)	**0.000**	**0.000**	**0.000**
	TPo*TPa	**0.000**	**0.000**	**0.000**
	TPo*AP	**0.000**	**0.000**	**0.000**
	TPa*AP	**0.000**	**0.000**	**0.000**
	TPo*TPa*AP	**0.000**	**0.000**	**0.000**
R^2 (adj)		99.99%	99.99%	99.72%
AD (P-Value ≥ 0.05)		0.099	0.199	0.101

Figure 7a (plot i) shows that the inclusion of particles provides small changes to the density of the epoxy; this is reasonable because the presence of cement particles leads to small variations of the density, and almost no change when rubber particles are used. Biopolymer, in contrast, shows a drastic drop in density due to the inclusion of the particles. The reduction is most evident when rubber particles are used (35% reduction in density); on the opposite, the presence of cement reduces the density by 14%. The two types of particles contribute to increase the biopolymer porosity due to the presence of bubbles during curing, which explains the significant decrease in density even with the use of cement particles. While the behaviour of the epoxy is unaffected by the quantity of particles used, the biopolymer shows instead a gradual decrease in density for larger amounts of particles (Figure 7a, plot ii). Different amounts of cement particles do not appear to affect the apparent density, however a significant change (8.5%) is observed from 3 wt% to 6/10wt% of rubber particles dispersed (Figure 7a, plot iii).

The apparent porosity and the water absorption are mutually dependent properties and they also present similar results. Samples that are more porous tend to absorb more water during saturation. The contribution given by the type of particles over the porosity is less evident for epoxy polymer. Figures 7b and 7c (plots i and ii) show some significant increases of the apparent porosity (from 2.2% to 28.7%) and water absorption (from 2.1% to 21.7%) when rubber particles are added to the biopolymer. A low amount of rubber (3 wt%) does not contribute to a significant change of the porosity and water

absorption of the biopolymer (Figure 7b and 7c, plot iii). On the other hand, cement particles generate slight changes of the porosity and water absorption (from 2.2% to 2.02% and from 2.1% to 1.93%, respectively, for 10 wt% cement inclusion). The effect of cement particles varies slightly between the high and low levels of the particle amount factor, but it is still significant according to Tukey's test.

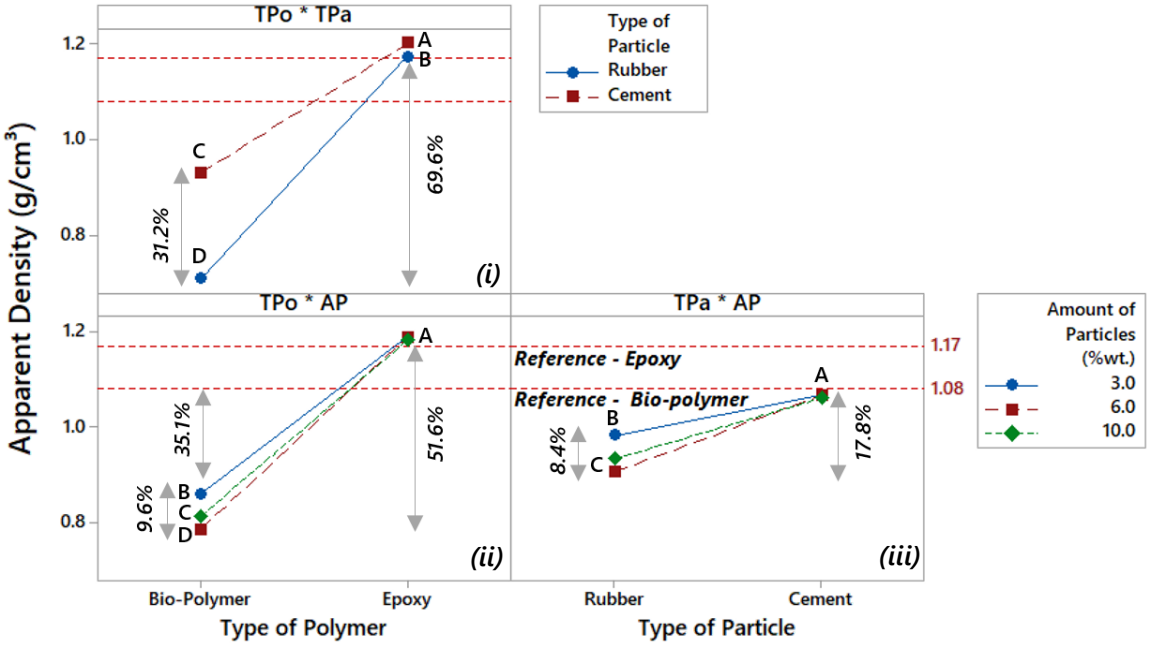

(a)

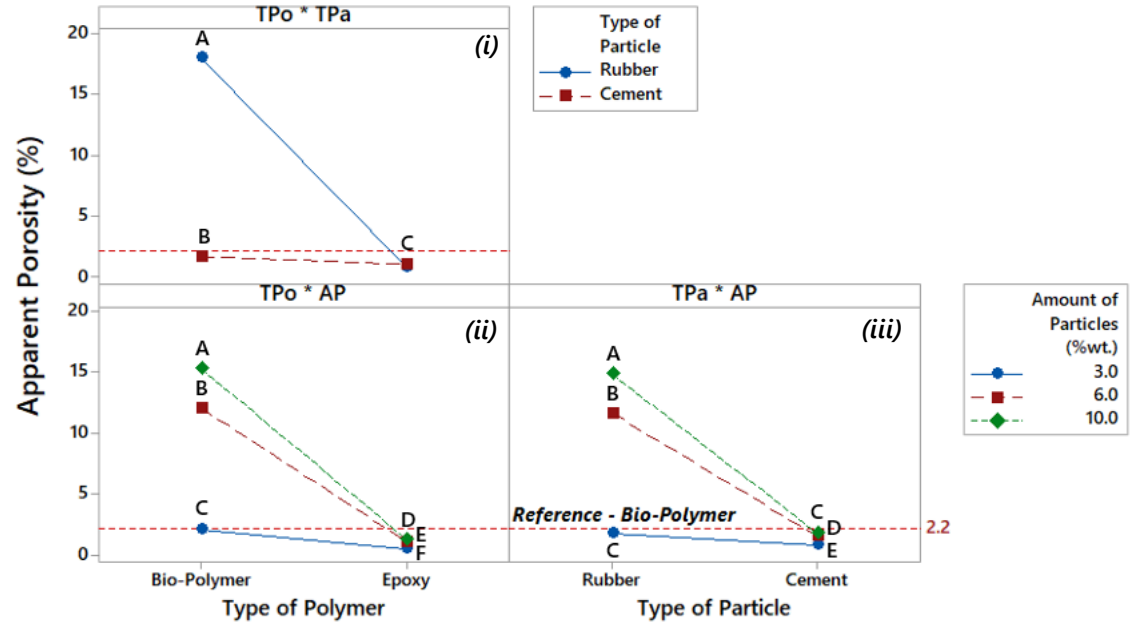

(b)

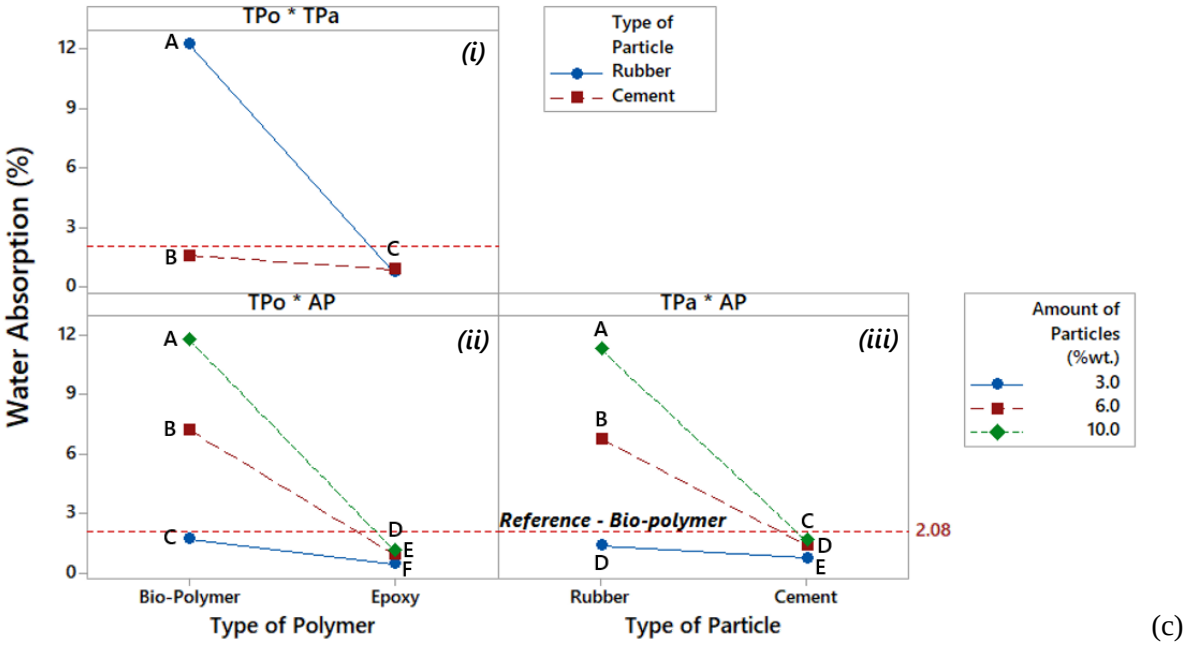

Figure 7. Third-order interaction plots for the apparent density (a), the apparent porosity (b) and the water absorption (c).

3.2 Bonding performance

Adhesion tests were performed on a set of reinforced polymers chosen on mechanical and physical results. The epoxy polymer and the biopolymer both provide an improvement of tensile strength, stiffness, impact resistance, porosity, water absorption and density with 3 wt% of particle inclusions. In this context, this particular amount of particles (3 wt%) was considered in a new design of experiment to evaluate the adhesive characteristics of polymers with aluminium (single lap test) and bottle caps (T-peel test) surfaces.

3.2.1 Single lap joint test

Table 7 shows the results of the single lap shear tests. A maximum coefficient of variation (CV) of 10.4% is obtained for the cement-reinforced epoxy polymer. Table 8 shows the Analysis of Variance (ANOVA) and the Anderson-Darling (AD) test results. R^2(adj) ranges from 98.78 to 98.95%, revealing a satisfactory adjustment to the model. The AD normality test also validates the ANOVA, showing P-values greater than 0.05. Second-order interaction effects are obtained for the three responses (P-values ≤ 0.05).

Table 7. Main Results for Single Lap shear Tests.

Type of Polymer	**Type of Particle**	**Amount of Particle (wt%)**	**Maximum load (N)**			**Apparent Shear Stress (MPa)**			**Single Lap Stiffness (10^6 N/m)**		
			Mean	SD	CV	Mean	SD	CV	Mean	SD	CV
Epoxy	-	-	1,303	96	7.4%	3.9	0.3	7.5%	7.1	0.5	7.6%
	Cement	3	1,206	125	10.4%	3.7	0.4	11.2%	8.0	0.6	8.1%
	Rubber	3	1,330	96	7.2%	4.2	0.4	10.0%	7.4	0.7	9.2%

Biopolymer	-	-	1,220	114	9.3%	3.8	0.4	9.2%	6.4	0.4	6.8%
	Cement	3	1,512	116	7.6%	4.7	0.4	8.8%	6.9	0.5	6.5%
	Rubber	3	1,600	127	8.0%	4.9	0.4	8.6%	6.6	0.6	9.3%
SD = standard deviation and CV = coefficient of variation											

Table 8. DoE Results for the tested conditions

Factors and Interactions		**Maximum load**	**Apparent Shear Stress**	**Single Lap Stiffness**
P-Value ≤ 0.05	Type of Polymer (TPo)	**0.000**	**0.000**	**0.000**
	Type of Particle (TPa)	**0.000**	**0.000**	**0.000**
	TPo*TPa	***0.000***	***0.000***	***0.005***
R^2 (adj)		98.78%	98.95%	98.94%
AD (P-Value ≥ 0.05)		0.487	0.844	0.525

Figures 8a and 8b show that the epoxy polymer has a 7% higher shear load than the biopolymer, while no significant change is observed for the apparent shear strength as the levels share the group letter C (Tukey test). The higher affinity of the biopolymer to the fillers significantly affects the maximum shear load of the reinforced polymers. The incorporation of particles into biopolymer provides a 30% increase of their maximum load, while a 7% reduction is observed for cement reinforced epoxy. Rubber inclusions do not present significant effects over the maximum load when epoxy is used. Moreover, cement and rubber particles show similar averages (Group A) when added to the biopolymer. A similar effect is also observed for the apparent shear stress, but with different percentage variations (Figure 8b). Although the presence of rubber particles enhances the shear strength of the epoxy by 7%, the use of cement particles contributes to a 5.5% reduction. Brittle adhesives tend to exhibit reduced shear lap strength due to decreased deformation and toughness. This conclusion can be confirmed by the interaction effect plot shown in Figure 8c, as the epoxy polymer features an 11% higher stiffness than the biopolymer in pristine conditions. The difference between the two polymers is even greater when they are reinforced with cement particles. In this case, a 15.5% increase is observed from epoxy to biopolymer. The incorporation of rubber and cement particles is beneficial for the two types of polymers tested, especially for epoxy.

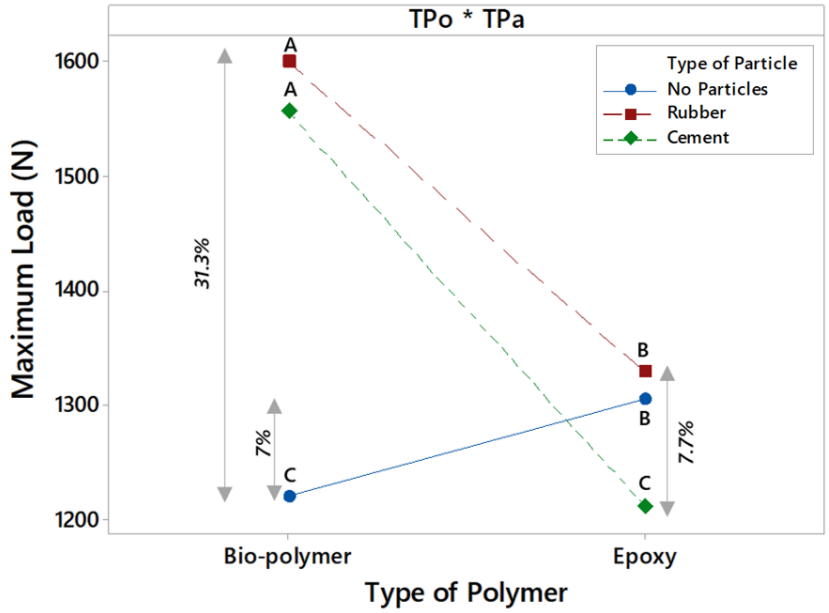
TPo * TPa
Type of Particle
No Particles
Rubber
Cement
Maximum Load (N)
1600
1500
1400
1300
1200
A
A
B
B
C
C
31.3%
7%
7.7%
Bio-polymer
Epoxy
Type of Polymer

(a)

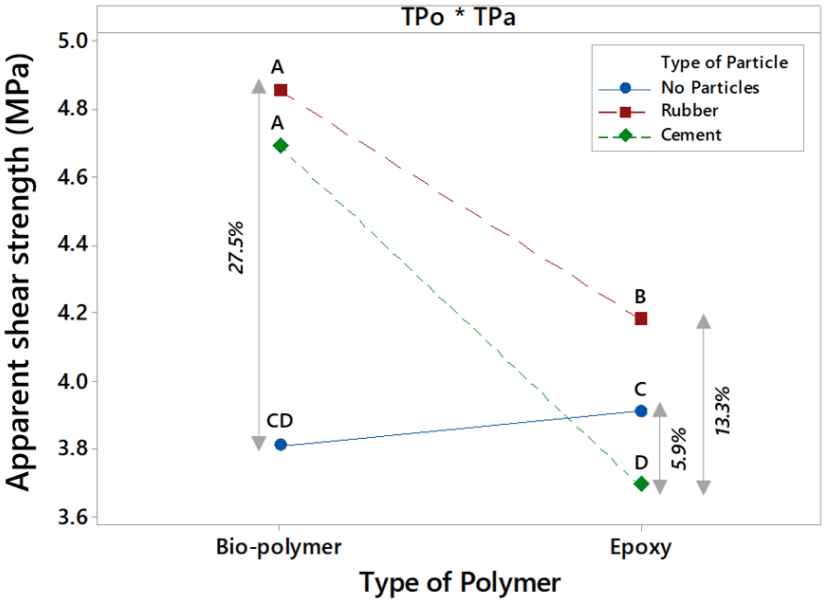
TPo * TPa
Type of Particle
No Particles
Rubber
Cement
Apparent shear strength (MPa)
5.0
4.8
4.6
4.4
4.2
4.0
3.8
3.6
A
A
B
C
CD
D
27.5%
5.9%
13.3%
Bio-polymer
Epoxy
Type of Polymer

(b)

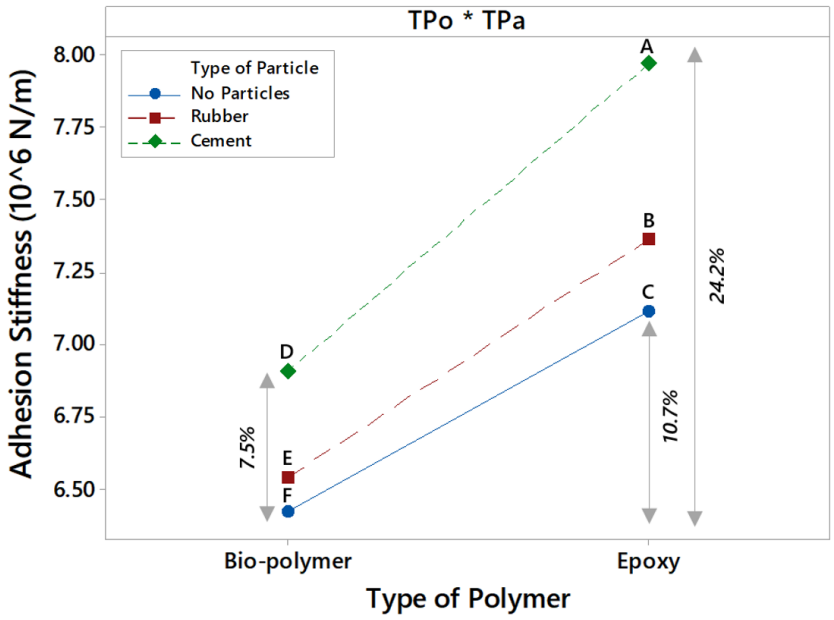

(c)

Figure 8. Interaction plots for maximum shear load (a), apparent shear strength (b) and apparent shear stiffness (c).

Figure 9 shows examples of the fractured area of single-lap samples after failure and the adhesive residue in the overlapped area. In general, brittle failure behaviour is most evident for epoxy polymer. Pristine epoxy shows both cohesive and adhesive failures (with an evident preponderance of adhesive failure), while the reinforced epoxy systems feature cracks of the adhesive surface that propagate perpendicular to the tensile load, leading to premature debonding of the polymer. The biopolymer also combines cohesive and adhesive failures, especially for pristine and rubber reinforced conditions. Cement particles provide similar behaviours found in epoxy polymer joints.

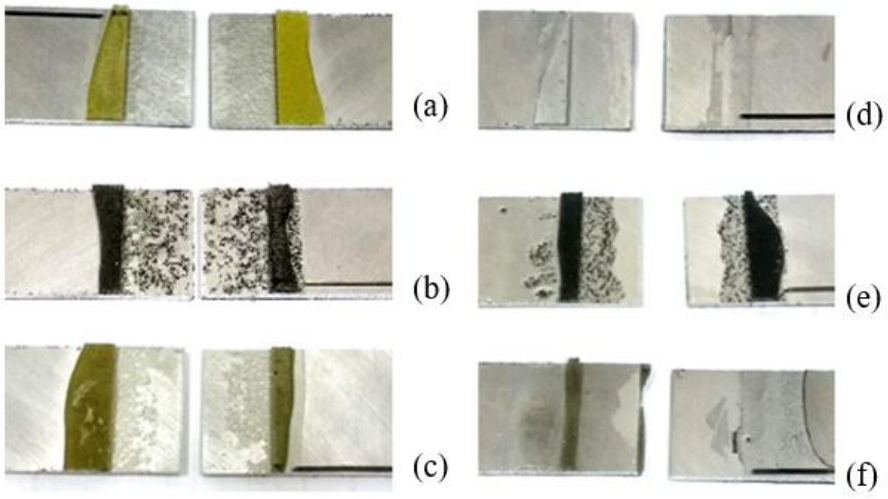

Figure 9. Failure mode analysis of biopolymer and epoxy, respectively, in pristine (a, b), with rubber particles (c, d), and with cement particles (e, f).

3.2.2 T-peel test

Table 9 shows the results for the adapted T-peel test between bottle caps and aluminium skins. The analysed properties are the peak load and the slope of the force vs. displacement curve in the region between 5 and 20 N. Peak loads are recorded according to the behaviour of T-peel test samples, which exhibited a short failure time, mainly for epoxy polymer. Biopolymer samples, on the other hand, show a progressive load until they reach the peak value. The coefficient of variation (CV) is limited to 9% for cement-reinforced biopolymer.

Table 9. Main Results for T-peel Tests.

Type of Polymer	Type of Particle	Amount of Particle (wt%)	Maximum Load (N)			Adhesion stiffness (10^3 N/m)		
			Mean	SD	CV	Mean	SD	CV
Epoxy	-	-	60.2	0.8	1.3%	33.5	1.4	4.1%
	Cement	3	60.8	0.5	0.8%	27.4	1.0	3.8%
	Rubber	3	48.7	3.0	6.2%	27.0	0.1	0.2%
Biopolymer	-	-	116.2	7.4	6.3%	35.5	1.1	3.0%
	Cement	3	82.4	7.5	9.0%	30.6	0.6	2.0%
	Rubber	3	85.3	0.8	0.9%	29.6	0.9	2.9%
SD = standard deviation and CV = coefficient of variation								

Table 10 shows the ANOVA and the normality test (AD) of the responses. A second order interaction effect is identified for the maximum peel load, while adhesion stiffness is affected only by the main factors. Figure 10 presents the interaction plot for maximum peel load and the main effect plot for adhesion stiffness. The adjustment of the experimental data for both responses is also satisfactory, with R^2 (adj) values ranging from 91.60% to 99.77%. P-Values greater than 0.05 calculated through the Anderson-Darling test validate the ANOVA.

Table 10. DoE Results for the tested conditions.

Factors and Interactions		Maximum load	Adhesion stiffness
P-Value ≥ 0.05	Type of Polymer (TPo)	**0.000**	**0.003**
	Type of Particle (TPa)	**0.000**	**0.000**
	TPo*TPa	**0.000**	0.705
R^2 (adj)		99.77%	91.60%
AD (P-Value ≥ 0.05)		0.919	0.928

The T-peel results confirm that the biopolymer described in this work provide a better bonding capacity than the epoxy polymer. The maximum load is 91% higher for the biopolymer than the epoxy in pristine conditions. However, a reduction in maximum load is obtained in the case of reinforced polymers, especially when biopolymer is used (26.5%). Biopolymer reinforced with rubber or cement exhibits similar loads, while epoxy shows a reduced resistance only when rubber particles are added. Similar findings are shown in Figure 10b for the adhesion stiffness. The biopolymer possesses a 9% greater bonding stiffness than the one exhibited by the epoxy polymer. The reinforcement is however not effective, reducing the stiffness by 16% (18%) when cement (rubber) particles are used. Note that

the cement and rubber particles have similar stiffness averages according to the Tukey test (i.e., same letter group B).

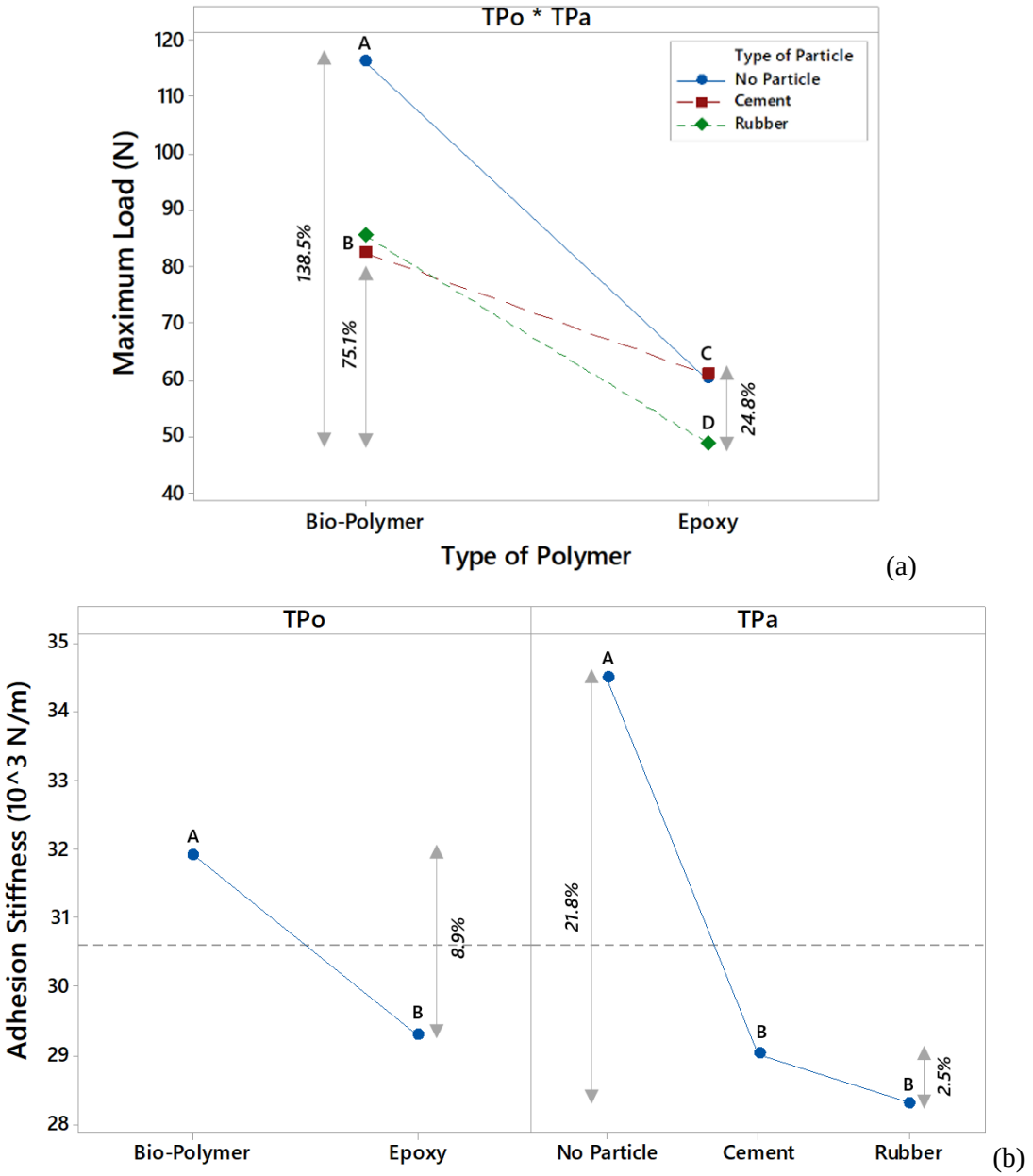

Figure 10. Interaction effect plot for the Maximum Peel load (a) and main effect plot for adhesion stiffness (b).

Figure 11 shows the mechanical behaviour (force vs displacement) of the polymers under peel loading. The epoxy polymer exhibits lower deformations compared to the biopolymer. In addition, brittle failures are most evident in the epoxy (i.e., sudden drops in load), which are caused by faster crack propagation within the polymer and subsequent debonding of the plastic caps. In contrast, the pristine biopolymer shows three distinct regions: (i) an initial elastic deformation followed by (ii) a plastic deformation with reduced load increment, and (iii) a long final deformation with a plateau close

to the peak load. At the end, a significant drop of the load is observed, indicating a progressive failure with large deformations.

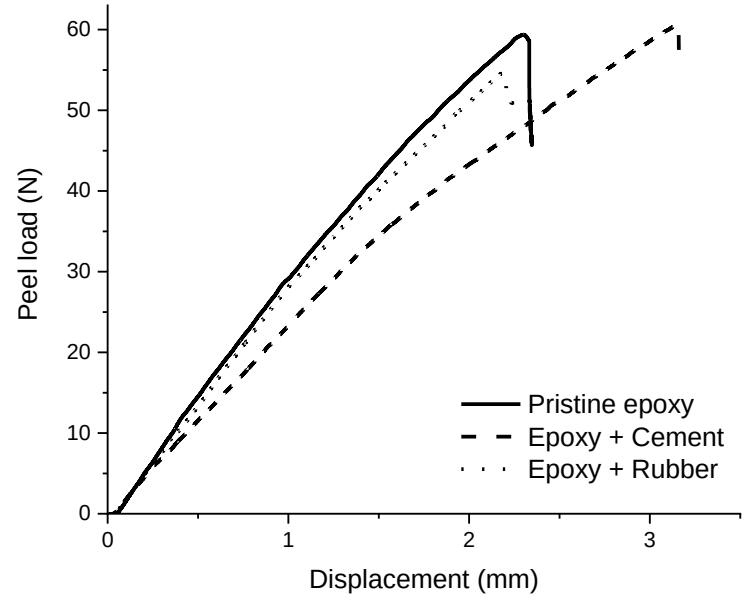

(a)

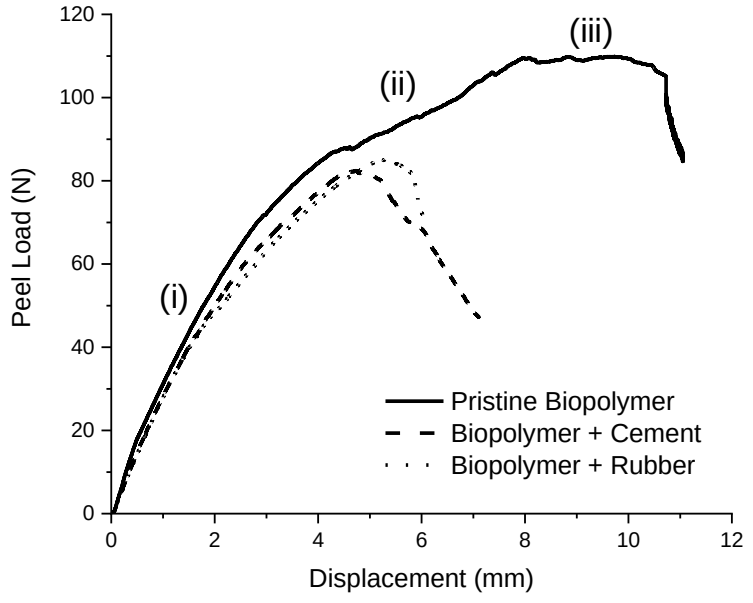

(b)

Figure 11. Force vs. displacement loads of T-peel tests with bottle caps for epoxy (a) and biopolymer adhesives (b)

3.3 SEM images

Figure 12 shows backscatter electron images of samples extracted from the fractured area of tensile dog-bone specimens for some of the conditions investigated in this work. Pristine biopolymer is compared to reinforced biopolymer with cement and rubber particles (Figures 12a to 12c). Reinforced epoxy is also shown in Figures 12d and 12e. A porous structure is observed for the biopolymer (Figure 12a), with pore sizes ranging from 30 to 400 µm. The cement and rubber particles are well distributed

in the biopolymer without apparent clusters. SEM images also reveal the increase in pore size (nearly 532 µm at 6 wt% of cement) when particles are added (Figure 12b), and this supports the conclusions from section 3.1.2, in which the incorporation of particles leads to enhanced apparent porosity of the biopolymer. Rubber particles also contribute to creating new pores and enlarging pore size in the structure (Figure 12c). In contrast, no macro pores are observed in the reinforced epoxy polymer. The bright areas in Figure 12d are indicative of a higher density material because of the presence of the cement particles. Rubber particles provide a good interface condition with epoxy matrix (Figure 12e).

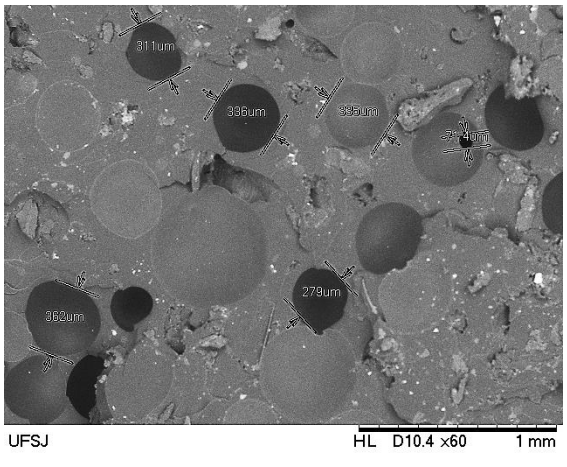

(a)

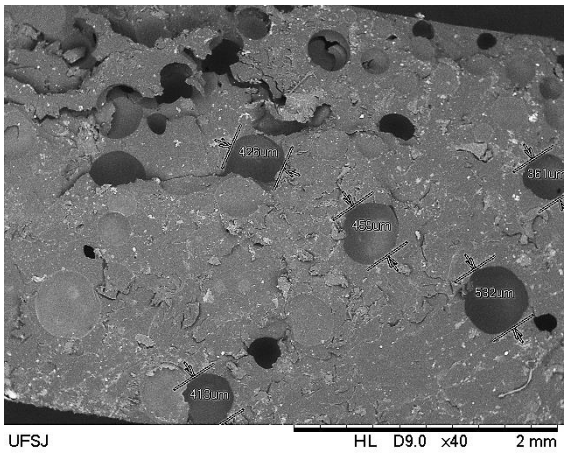

(b)

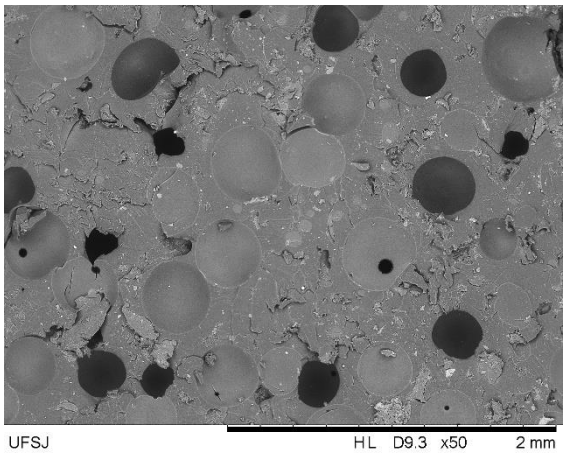

(c)

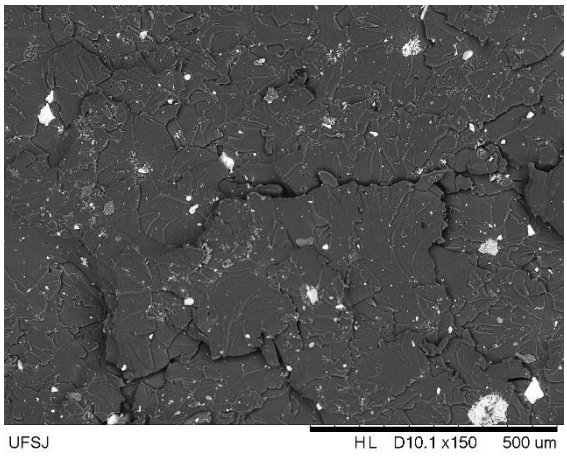

(d)

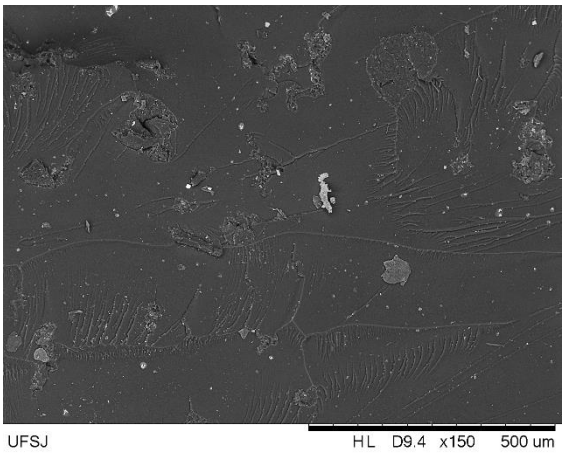

(e)

Figure 12. SEM images of pristine biopolymer (a), biopolymer with 6 wt% cement (b), biopolymer with 10 wt% rubber (c), epoxy with 3 wt% cement (d), and epoxy with 10 wt% rubber (e).

3.4 Additional comments

Table 11 shows a summary of the main mechanical and physical properties of epoxy and bio polymer compositions, considering only the 3 wt% of particles. From a qualitative perspective the use of particles has a more pronounced effect in biopolymer adhesives. Cement particles provide larger increases of the biopolymer mechanical properties and bond strength, while rubber causes a slight reduction of the mechanical properties, but an increased bond strength. In contrast - and depending on the type of particles used - the reinforced epoxy exhibits moderate changes in responses because of the reduced affinity with the fillers. It is noteworthy that the impact resistance of reinforced epoxy polymer is reduced, especially with rubber particles, while biopolymer exhibits moderate to significant increments for both fillers.

Table 11. Summary of the effects of the treatments over the properties considered in this work.

Type of Polymer	Type of Particle	Amount of Particle (wt%)	Young's Modulus	Tensile Strength	Impact Resistance	Apparent Density	Apparent Porosity	Single lap Strength	Max. Peel load
Biopolymer	Cement	3	++	++	++	-	+	++	-
Biopolymer	Rubber	3	--	--	+	--	++	++	-
Epoxy	Cement	3	+	+	-	+	+	+	O
Epoxy	Rubber	3	O	-	--	O	+	-	-

(++: High increment, +: Moderate increment, O: marginal modification, -: low reduction, --: significant reduction)

4. Conclusion

Castor-oil-based biopolymer has been proposed here as an alternative adhesive for bonding metal skins to polymer bottle caps, producing therefore a eco-friendly structural sandwich panel. A comparison of a bio-polyurethane from castor oil plant with a commercial polymer was performed by testing a commonly used epoxy polymer as adhesive. The conclusions one can draw from this work are:

i. The dispersion of cement leads to increased tensile strengths and stiffness in both polymers. The biopolymer achieves a 55% increase in tensile strength and 183% in stiffness. In contrast, rubber particles significantly reduce the strength of the biopolymer strength, while the epoxy is barely affected by the presence of rubber;

ii. Reinforced biopolymer provides increased impact resistance, reaching 72% for cement and 7.5% for rubber particles, while epoxies show some significant reductions attributed to lower particle affinity;

iii. Higher amounts of particles contribute to decrease the biopolymer density attributed to the increased porosity level. Low density and acceptable porosity level are achieved with 3 wt% of

cement in biopolymers. The epoxy polymer achieves a slight increase in density and porosity by the inclusion of particles;

iv. Reinforced biopolymer features a 28% increase in apparent shear strength, while epoxy polymers have higher shear strength only when rubber particles are added. Cohesive failures are predominant in biopolymer samples, while major adhesive failures are evidenced in bonded epoxy joints;

v. Higher peel resistance and stiffness are obtained by biopolymer tested compared to epoxy polymer. In contrast, particle incorporation reduces peel loads for both polymers. The force vs. displacement plots indicate a more ductile and progressive failure when biopolymers are used.

Despite their reduced strength and stiffness compared to epoxy, the reinforced biopolymer tested appears to be a promising adhesive for sustainable structural constructions, with enhanced shear and peel strength and adequate tensile strength and stiffness. This adhesive is adequate for using in eco-friendly secondary structures to provide a feasible route to reuse plastic disposals in the automotive and construction engineering, indicating a promising use of biobased adhesives when particle reinforcement is applied. Further investigations will be conducted on "Life Cycle Assessment" of sustainable panels.

ACKNOWLEDGMENT

The authors acknowledge the support of CNPq-Brazil (PhD scholarship 290224/2017-9, PDE - 205255/2017-5) in this project and the donation of the biopolymer by Imperveg Ltda (Brazil).

DECLARATION OF INTERESTS

The authors declare that there is no conflict of interest.

REFERENCES

1. Saraç I, Adin H, Temiz Ş. Experimental determination of the static and fatigue strength of the adhesive joints bonded by epoxy adhesive including different particles. Composites Part B: Engineering 2018; 155:92–103. doi:10.1016/j.compositesb.2018.08.006.

2. Zhou H, Liu H-Y, Zhou H, Zhang Y, Gao X, Mai Y-W. On adhesive properties of nano-silica/epoxy bonded single-lap joints. Materials & Design 2016; 95:212–8. doi:10.1016/j.matdes.2016.01.055.

3. Jojibabu P, Jagannatham M, Haridoss P, Ram GJ, Deshpande AP, Bakshi SR. Effect of different carbon nano-fillers on rheological properties and lap shear strength of epoxy adhesive joints. Composites Part A: Applied Science and Manufacturing 2016; 82:53–64. doi:10.1016/j.compositesa.2015.12.003.

4. Scarselli G, Corcione C, Nicassio F, Maffezzoli A. Adhesive joints with improved mechanical properties for aerospace applications. International Journal of Adhesion and Adhesives 2017; 75:174–80. doi:10.1016/j.ijadhadh.2017.03.012.

5. Quan D, Carolan D, Rouge C, Murphy N, Ivankovic A. Mechanical and fracture properties of epoxy adhesives modified with graphene nanoplatelets and rubber particles. International Journal of Adhesion and Adhesives 2018; 81:21–9. doi:10.1016/j.ijadhadh.2017.09.003.

6. Santana PRT, Panzera TH, Freire RTS, Christoforo AL. Apparent shear strength of hybrid glass fibre reinforced composite joints. Polymer Testing 2017; 64:307–12. doi:10.1016/j.polymertesting.2017.10.022.

7. Packham D. Adhesive technology and sustainability. International Journal of Adhesion and Adhesives 2009; 29:248–52. doi:10.1016/j.ijadhadh.2008.06.002.

8. Moghadam PN, Yarmohamadi M, Hasanzadeh R, Nuri S. Preparation of polyurethane wood adhesives by polyols formulated with polyester polyols based on castor oil. International Journal of Adhesion and Adhesives 2016; 68:273–82. doi:10.1016/j.ijadhadh.2016.04.004.

9. Tenorio-Alfonso A, Pizarro M, Sánchez M, Franco J. Assessing the rheological properties and adhesion performance on different substrates of a novel green polyurethane based on castor oil and cellulose acetate: A comparison with commercial adhesives. International Journal of Adhesion and Adhesives 2018; 82:21–6. doi:10.1016/j.ijadhadh.2017.12.012.

10. Malik M, Kaur R. Mechanical and Thermal Properties of Castor Oil-Based Polyurethane Adhesive: Effect of TiO2 Filler. Advances in Polymer Technology 2016; 37:24–30. doi:10.1002/adv.21637.

11. Panchireddy S, Grignard B, Thomassin J-M, Jerome C, Detrembleur C. Biobased poly(hydroxyurethane) glues for metal substrates. Polymer Chemistry 2018; 9:2650–9. doi:10.1039/c8py00281a.

12. Oliveira PR, Bonaccorsi AMS, Panzera TH, Christoforo AL, Scarpa F. Sustainable sandwich composite structures made from aluminium sheets and disposed bottle caps. Thin-Walled Structures 2017; 120:38–45. doi:10.1016/j.tws.2017.08.013.

13. Oliveira PR, Panzera TH, Freire RT, Scarpa F. Sustainable sandwich structures made from bottle caps core and aluminium skins: A statistical approach. Thin-Walled Structures 2018; 130:362–71. doi:10.1016/j.tws.2018.06.003.

14. Filho SLMR, Oliveira PR, Panzera TH, Scarpa F. Impact of hybrid composites based on rubber tyres particles and sugarcane bagasse fibres. Composites Part B: Engineering 2019; 159:157–64. doi:10.1016/j.compositesb.2018.09.054.

15. Montgomery DC. Introduction to statistical quality control. USA: Wiley; 1997.

16. ASTM D638-14, Standard Test Method for Tensile Properties of Plastics. West Conshohocken – PA: ASTM International; 2014.

17. ASTM D6110-10, Standard Test Method for Determining the Charpy Impact Resistance of Notched Specimens of Plastics. West Conshohocken – PA: ASTM International; 2010.

18. ASTM C20-15, Standard Test Methods for Apparent Porosity, Water Absorption, Apparent Specific Gravity, and Bulk Density of Burned Refractory Brick and Shapes by Boiling Water. West Conshohocken – PA: ASTM International; 2015.

19. ASTM D1002-10, Standard Test Method for Apparent Shear Strength of Single-Lap-Joint Adhesively Bonded Metal Specimens by Tension Loading (Metal-to-Metal. West Conshohocken – PA: ASTM International; 2010.

20. Mousa S, Kim G-Y. A direct adhesion of metal-polymer-metal sandwich composites by warm roll bonding. Journal of Materials Processing Technology 2017; 239:133–9. doi:10.1016/j.jmatprotec.2016.08.017.